Post-plasma carbon bed design for CO_2 conversion: Does size and insulation matter?

Colin O'Modhrain*, Yury Gorbanev, Annemie Bogaerts

Research group PLASMANT, Department of Chemistry, University of Antwerp, Universiteitsplein 1, 2610 Wilrijk, Belgium

*Corresponding author.

E-mail address: colin.omodhrain@uantwerpen.be (C. O'Modhrain)

Supporting information

Table of Contents

Section S1. Additional experimental details

The unit of flow rate was set according to the Bronkhorst standard litre per minute, which aligns with the standard EU definition taken at 293 K and 1 atm (molar volume = 24.06 L/mol). Due to the constriction of the reactor outlet, a reverse vortex flow pattern develops within the reactor chamber, as detailed in previous works from our group [1-3].

At the lower end of SEI (i.e. higher flow rate), the plasma may exhibit some restriking behaviour, increasing the random nature of the peaks and reducing the plasma stability. This was avoided as best as possible, resulting in some minor deviation in SEI between the configurations. The current was varied between the conditions and beds to allow for SEI matching, meaning that the ratio of power to flow rate was relatively constant between the beds.

The outlet of each bed was equipped with a fine metallic mesh to keep carbon within. In addition, a small sacrificial mesh was placed over the anode to prevent carbon from entering into the reactor.

Fig. S1. An example oscillogram demonstrating the plasma operating in takeover mode

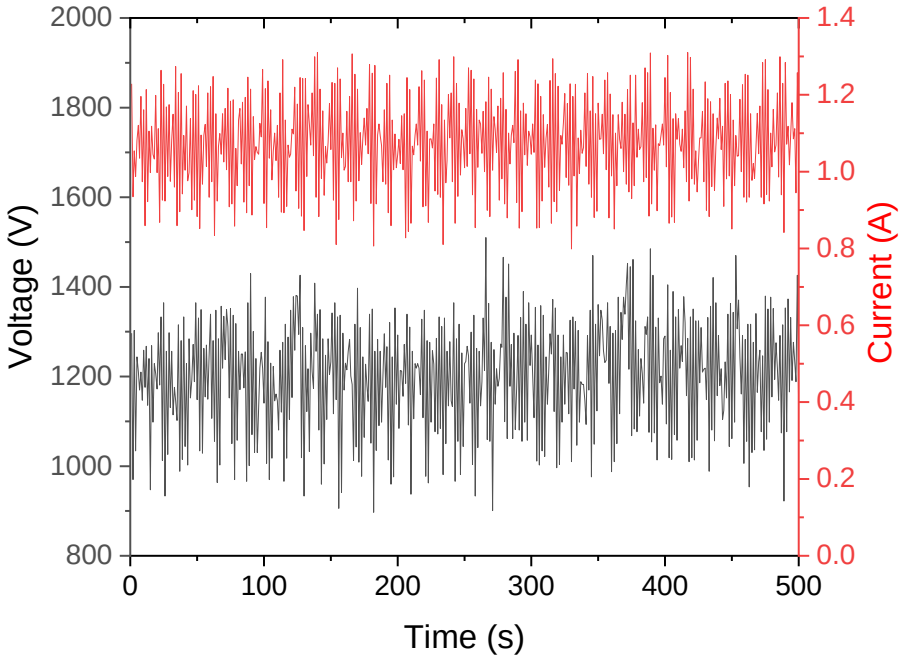

Electric arcs typically exist in one of three modes; steady, takeover and restrike [4]. In the steady mode, voltage and current fluctuations are minimal and the signal is relatively constant. In the takeover more, more quasi-periodic fluctuations appear in the waveforms, as demonstrated in the figure above. Finally, the restriking mode is characterized by chaotic and non-periodic voltage and current temporal variations. In our experiments, the arc fluctuations (and hence voltage and current variations) were quasi-periodic, thus characterizing our mode of operation as the takeover mode.

Fig. S2. Experimental setup for heated external silo tests, implemented with the long carbon bed.

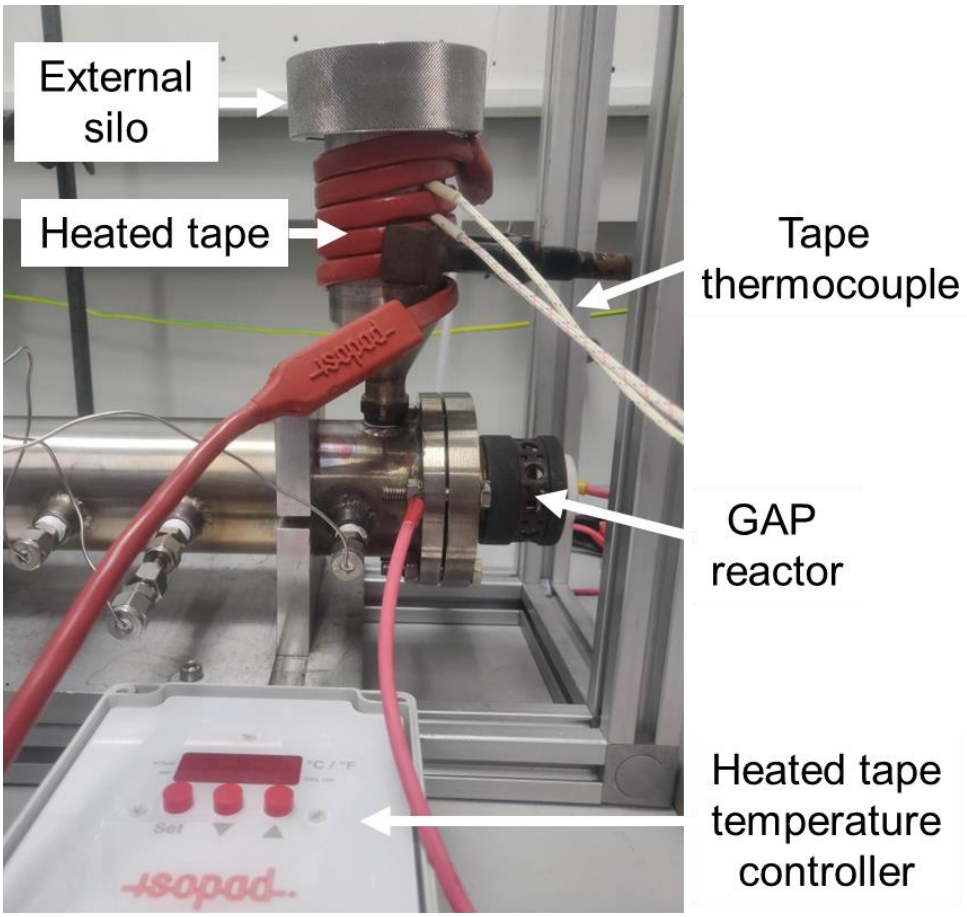

Section S2. Formulae for energy efficiency derived by Huang *et al.* [5] and Zhang *et al.* [6]

Huang *et al.* and Zhang *et al.* derived the following formulae to determine the contribution of plasma-based CO_2 dissociation and reverse Boudouard reaction (RBR) towards the calculation of energy efficiency (EE) of the system. The oxygen balance was used to determine said contributions.

$$\alpha_{CO_2\ dissociation}\,(\%) = \frac{2 * y_{O_2}^{out}}{2 * y_{O_2}^{out} + \frac{1}{2} * \left(y_{CO}^{out} - 2 * y_{O_2}^{out}\right)} * 100\% \qquad (SE1)$$

$$\alpha_{RBR}(\%) = \frac{\frac{1}{2} * \left(y_{CO}^{out} - 2 * y_{O_2}^{out}\right)}{2 * y_{O_2}^{out} + \frac{1}{2} * \left(y_{CO}^{out} - 2 * y_{O_2}^{out}\right)} * 100\% \qquad (SE2)$$

In these equations, the factor α represents the contribution of the relative reaction shown in subscript (value = 0-1) and γ represents the fraction of the component indicated in subscript (i.e. CO_2/CO/O_2) detected at the outlet.

If the fraction of O_2 detected at the outlet is equal to zero, as is often the case in works regarding post-plasma carbon beds, then the contribution of plasma-based CO_2 dissociation ($\alpha_{CO_2\ \text{dissociation}}$, SE1) also becomes zero. This results in the standard reaction enthalpy of the RBR being the sole reaction contributing to the calculation of EE, which results in an underestimation ($\Delta H_{r\ RBR}^{\circ} < \Delta H_{r\ CO_2\ dissociation}^{\circ}$).

Section S3. Numerical example of energy efficiency calculation, showing the effect of various assumptions

Two main reactions contribute to the conversion of CO_2 in a system incorporating a post-plasma carbon bed, i.e., the plasma-based decomposition of CO_2 (SR1), and the RBR (SR2):

$$CO_2(g) \rightleftharpoons CO(g) + \frac{1}{2}O_2(g) \qquad \Delta H_r^\circ = +283\ kJ/mol \qquad SR1$$

$$CO_2(g) + C(s) \rightleftharpoons 2CO(g) \qquad \Delta H_r^\circ = +172.5\ kJ/mol \qquad SR2$$

Additionally, three more reactions can occur between the oxygen produced by the CO_2 plasmolysis and the carbon present inside the bed.

$$O_2(g) + 2C(s) \rightarrow 2CO(g) \qquad SR3$$

$$O_2(g) + C(s) \rightarrow CO_2(g) \qquad SR4$$

$$O(g) + C(s) \rightarrow CO(g) \qquad SR5$$

In Section 3 in the main text, we made the assumption that only reaction SR3 occurs and the contribution of SR4 is negligible. The following example will demonstrate the influence of this assumption on the conversion and energy efficiency. In both cases, SR5 is assumed to be occurring in equal amounts at a specific SEI. As such, this reaction has been neglected in the following examples.

Conversion

We assume an inlet flow rate of 10 L/min CO_2 and the following gas concentrations are detected in the effluent stream:

$$CO_2 = 60\ \%\quad CO = 40\ \%\quad O_2 = 0\ \%$$

We also assume that one liter of CO_2 is converted due to the plasma, which corresponds to a plasma-based conversion of 10 %. In this scenario, we can calculate the amount of CO_2 converted by the RBR for two distinct cases.

Case 1: SR3 is dominant solid carbon oxidation with O_2 in the carbon bed

$$y_{CO_2}^{out} = 0.6 = \frac{y_{CO_2}^{out}}{y_{CO}^{out} + y_{CO_2}^{out} + y_{O_2}^{out}} = \frac{9 - \chi}{1 + 1 + 2\chi + 9 - \chi + 0} => \chi = 1.5\ L$$

From the 9 litres of CO_2 left after conversion by the plasma, χ litres are converted by the RBR. One litre of CO was formed by the plasma, and one litre was formed via reaction SR3. 2χ more litres will be formed via the RBR. This results in 1.5 L of CO_2 converted by the RBR. This corresponds to a net total amount of CO_2 converted of 2.5 L, or 25 % (1 L from the plasma and 1.5 L from RBR). The same can be done for case 2:

Case 2: SR4 is dominant solid carbon oxidation with O_2 in the carbon bed

$$y_{CO_2}^{out} = 0.6 = \frac{y_{CO_2}^{out}}{y_{CO}^{out} + y_{CO_2}^{out} + y_{O_2}^{out}} = \frac{9 - \chi + 0.5}{1 + 2\chi + 9 - \chi + 0.5 + 0} => X = 2\ L$$

The biggest difference is that the oxygen produced by the plasma reaction (SR1) does not produce CO, but CO_2. However, this case also results in a net total CO_2 conversion of 2.5 L (25 %): one litre removed by the plasma, 2 litres removed by the RBR, and half a litre produced by reaction SR4.

Energy efficiency

The energy efficiency can be calculated via the following formula:

$$EE(\%) = \frac{\chi_{total}(\%) * \left(\alpha_{Plasma} * \Delta H^{\circ}_{r,Plasma}(kJ/mol) + \alpha_{RBR} * \Delta H^{\circ}_{r,RBR}(kJ/mol)\right)}{SEI\ (kJ/mol)}$$

Hence, the contribution of both the plasma and RBR to the total CO_2 conversion must be determined.

$$\alpha_{Plasma} = \frac{\chi_{plasma}(\%)}{\chi_{total}(\%)}$$

$$\alpha_{RBR} = 1 - \alpha_{Plasma}$$

Case 1:

$$\alpha_{Plasma} = \frac{\chi_{plasma}(\%)}{\chi_{total}(\%)} = \frac{1\ L}{2.5\ L} = 0.4$$

$$\alpha_{RBR} = 1 - \alpha_{Plasma} = 1 - 0.4 = 0.6$$

If we take the high SEI value, we get:

$$EE(\%) = \frac{25\% * \left(0.4 * \frac{283kJ}{mol} + 0.6 * \frac{172.5kJ}{mol}\right)}{\frac{164kJ}{mol}} = 33.1\%$$

Case 2:

Because the plasma-based CO_2 conversion facilitates reaction SR4 by being responsible for the production of oxygen, its contribution to the overall conversion will be lower.

$$\alpha_{Plasma} = \frac{\chi_{plasma}(\%)}{\chi_{total}(\%)} = \frac{1\ L - 0.5\ L}{2.5\ L} = 0.2 \quad (39)$$

$$\alpha_{RBR} = 1 - \alpha_{Plasma} = 1 - 0.2 = 0.8 \tag{40}$$

This results in the following energy efficiency:

$$=> EE(\%) = \frac{25\% * \left(0.2 * \frac{283kJ}{mol} + 0.8 * \frac{172.5kJ}{mol}\right)}{\frac{115kJ}{mol}} = 29.7\% \tag{41}$$

Depending on the assumption made, a difference of about 5 % can occur.

In reality a combination of both reaction SR3 and SR4 will occur simultaneously. However, detecting the specific reaction occurring would be highly complex and outside the scope of this work.

Fig. S3. Example of (a) CO_2, CO and O_2 concentration profiles during an experiment and (b) example of a conversion profile with the pseudo-steady-state region highlighted.

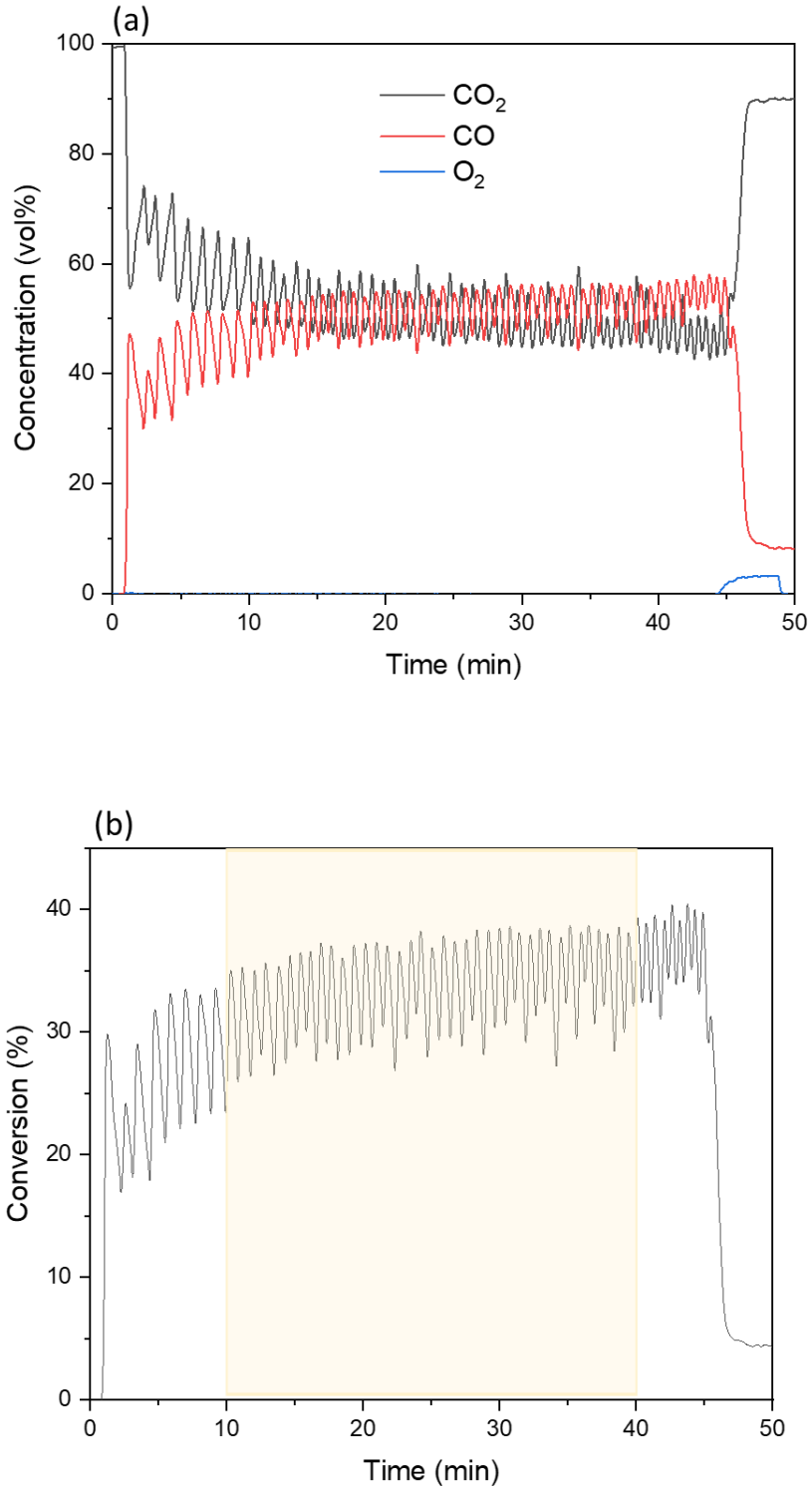

Table S1. Carbon loading and remaining post-reaction

Bed	Flow rate (L/min)	SEI (kJ/L)	Carbon loading (g)	Carbon remaining post-reaction (g)	Carbon reacted (%)
Short	10	6.8	80	2.3	97
	20	3.7		1.9	98
Long	10	6.8		2.5	97
	20	3.7		2.8	97
Insulated	10	6.8		2.2	97
	20	3.7		2.4	97

Table S2. Average contribution factors ($\alpha_{CO_2\ dissociation}$ & α_{RBR}) for all studied conditions

Bed	Carbon present?	Flow rate (L/min)	SEI (kJ/L)	$\alpha_{CO_2\ dissociation}$	α_{RBR}
Short	Y	10	6.8	0.40	0.60
	N	10	6.8	1.0	0.0
	Y	20	3.7	0.61	0.39
	N	20	3.7	1.0	0.0
Long	Y	10	6.8	0.23	0.77
	N	10	6.8	1.0	0.0
	Y	20	3.7	0.51	0.49
	N	20	3.7	1.0	0.0
Insulated	Y	10	6.8	0.48	0.52
	N	10	6.8	1.0	0.0
	Y	20	3.7	0.65	0.35
	N	20	3.7	1.0	0.0

Section S4. Analysis of insulated bed conversion and energy metrics

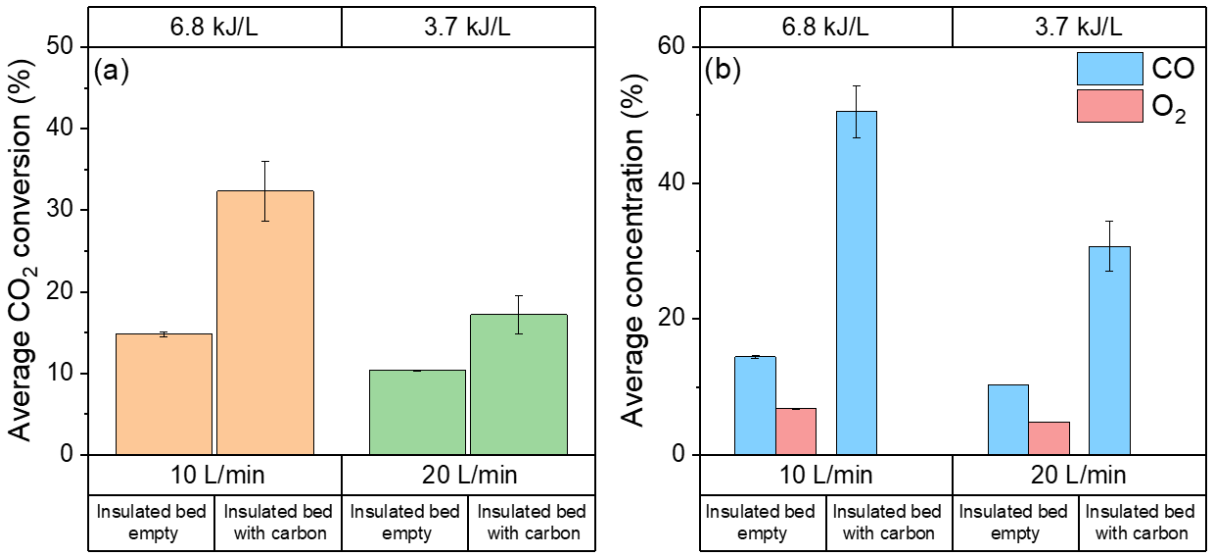

Fig. S4. Comparison of (a) average CO_2 conversion and (b) CO and O_2 concentrations for the insulated bed, when empty and filled with carbon, at high (6.8 kJ/L) and low (3.7 kJ/L) SEI values.

In terms of conversion, the insulated bed performs in-line with the short bed at high SEI (**Error! Reference source not found.**a above), reaching an average conversion of 32 % compared to 34 % obtained with the short bed. At low SEI, the values fall in-line with those obtained for both the short and long bed, with a slightly lower average value of 17 % (versus 20 % with the short bed and 19 % with the long bed). The slight reduction in conversion performance compared to the previous two beds is likely due to the fact that the plasma afterglow is not in direct contact with the carbon in the insulated bed. This change leads to a longer distance required for O/O_2 species to travel prior to interaction with the carbon, resulting in a larger extent of recombination of O/O_2 with CO instead of reacting with solid carbon [7,8]. In terms of the difference between high and low SEI, the insulated bed volume is similar to that of the short bed, meaning that the heat and species flux out of the reactor is more significant than with the long bed.

The performance enhancement is more pronounced at high SEI, yielding a factor two improvement in CO_2 conversion, and a factor three in CO concentration (Fig. 7b). Furthermore, the insulated carbon bed can also completely remove the produced O_2, both at high and low SEI (Fig. 7b), thus significantly reducing separation costs.

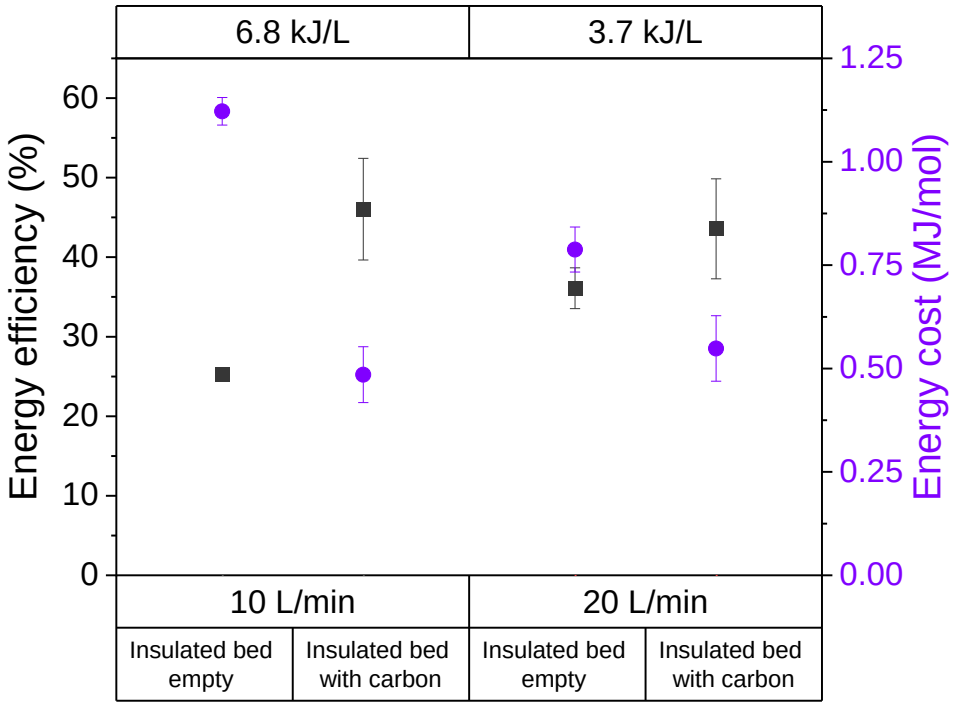

Fig. S5. Comparison of energy cost and energy efficiency between empty and filled insulated carbon bed at high (6.8 kJ/L) and low (3.7 kJ/L) SEI values.

The EE and EC of the insulated bed at high and low SEI conditions, for both empty bed and filled with carbon are plotted in Fig. . As observed with the short and long beds, the introduction of carbon results in improved energy metrics (both EE and EC) at the same SEI condition. Decreasing SEI in the presence of carbon reduces the performance marginally, resulting in a drop in EE from 46 % to 44 % and a rise in EC from 0.49 MJ/mol to 0.55 MJ/mol. This rise in EC (and drop in EE) is because the drop in conversion (from 32 % to 17 %) is relatively larger than the drop in SEI (see **Error! Reference source not found.** 12).

In comparison to the short and long beds, the insulated bed performs slightly better than the short bed at high SEI, reaching an EE of 46 % (compared to 41 %). This value is still below the maximum EE for the long bed (51 %) at high SEI. In terms of EC, both low and high SEI conditions with the insulated bed yield a higher value than the other two designs. The EC at high SEI is 0.49 MJ/mol, slightly higher than for the short bed. At low SEI, an EC of 0.55 MJ/mol is obtained, which is higher than for the other investigated configurations. This can be attributed to the lower conversion obtained with this bed at low SEI.

The discrepancy in EE and EC comparison between the short and insulated bed noticeable at high SEI is due to a multitude of minor differences in each of the variables required to calculate EE. Primarily, the CO_2 dissociation contribution (see SI, Table S1) in the insulated bed (0.46) is slightly higher than the same value in the short bed (0.4), which increases the EE. This difference in the relative values of EE and EC for the short and insulated beds further highlights the fact that calculating the EE in a multi-reactant system is heavily influenced by the variables, their derivation, and the assumptions therein. As such, EE is decidedly not the most suitable energy metric for accurately analysing the performance of a system containing a post-plasma carbon bed (and other complex multi-reactant systems such as plasma-based dry reforming of methane [9,10]). We advocate for the use of EC as the key metric for comparing energy performance results obtained within a study, and also between published works.

Fig. S6. Graphical example of potential long bed silo coupling redesign with aim of reducing fresh carbon impinging on plasma arc/afterglow.

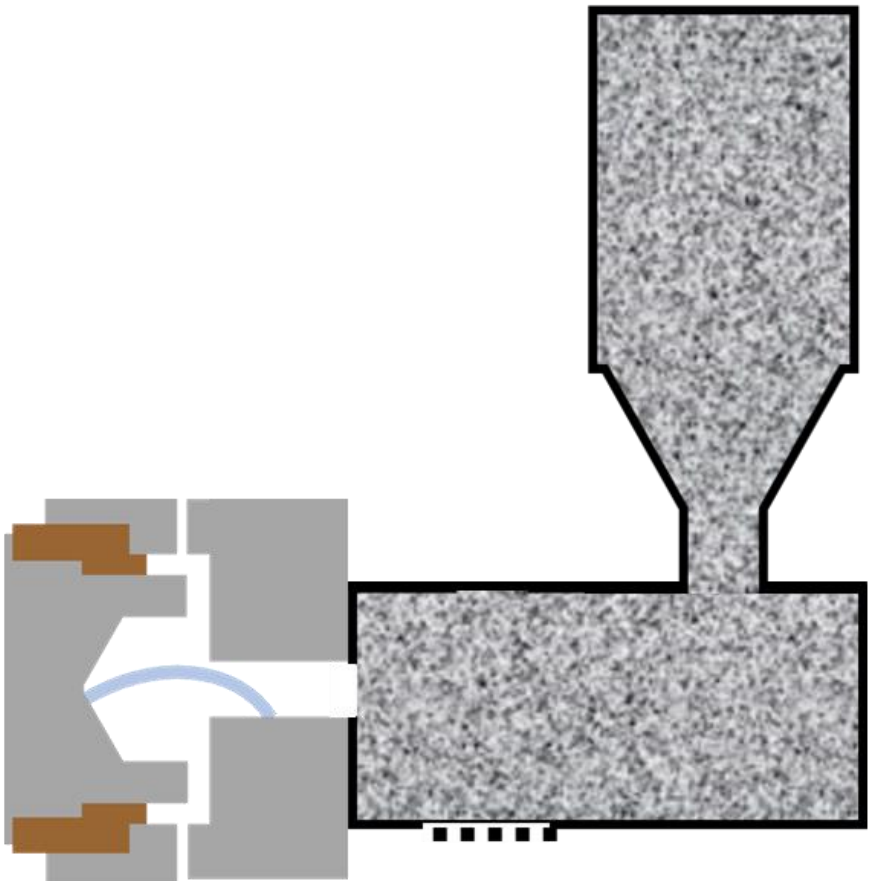

References

[1] R. Vertongen and A. Bogaerts, Journal of CO2 Utilization 72 (2023) 102510-102531
[2] G. Trenchev, S. Kolev, W. Wang, M. Ramakers, and A. Bogaerts, Journal of Physical Chemistry C 121 (2017) 24470-24479
[3] M. Ramakers, G. Trenchev, S. Heijkers, W. Wang, and A. Bogaerts, ChemSusChem 10 (2017) 2642-2652
[4] S. A. Wutzke, E. Pfender, and E. R. G. Eckert, Aiaa Journal 5 (1967) 707-&
[5] J. Y. Huang, H. Zhang, Q. H. Tan, L. Li, R. Y. Xu, Z. M. Xu, and X. D. Li, Journal of Co2 Utilization 45 (2021)
[6] H. Zhang, Q. H. Tan, Q. X. Huang, K. Y. Wang, X. Tu, X. T. Zhao, C. F. Wu, J. H. Yan, and X. D. Li, Acs Sustainable Chemistry & Engineering 10 (2022) 7712-7725
[7] F. A. D'Isa, E. A. D. Carbone, A. Hecimovic, and U. Fantz, Plasma Sources Science and Technology 29 (2020)
[8] Y. Wu, S. Z. Li, Y. L. Niu, H. J. Yan, D. Z. Yang, and J. L. Zhang, Journal of Physics D-Applied Physics 56 (2023) 065201-065214
[9] N. Pinhão, A. Moura, J. B. Branco, and J. Neves, International Journal of Hydrogen Energy 41 (2016) 9245-9255
[10] B. Wanten, S. Maerivoet, C. Vantomme, J. Slaets, G. Trenchev, and A. Bogaerts, Journal of CO2 Utilization 56 (2022) 101869-101880